# Gas or Liquid? The Supercritical Behavior of Pure Fluids

Elizabeth A. Ploetz and Paul E. Smith*

Department of Chemistry, Kansas State University, 213 CBC Building, 1212 Mid Campus Dr. North, Manhattan, Kansas 66506-0401, United States

S *Supporting Information*

ABSTRACT: By definition, the distinction between a gas and a liquid ceases to exist beyond the critical point for pure fluids. Nevertheless, there remains a strong desire to attribute gas-like or liquid-like behavior to fluids corresponding to different parts of the supercritical region, especially as this becomes important for understanding and designing the properties of supercritical fluids. Here, we use a combination of fluctuation solution theory and accurate equation of state data to elucidate an easily accessible dividing line and corresponding transition regime between liquid-like and gas-like behavior in the supercritical region of all pure fluids. Liquid-like behavior in the supercritical region is characterized by a negative skewness in the particle number distribution for an equivalent open system, indicating that particle deletion is favored for liquids, whereas gas-like behavior is characterized by a positive skewness, indicating that particle insertion is favored for gases. Identical behavior is observed either side of the liquid−vapor line. The possible consequences for the behavior of fluids at the critical point are also discussed.
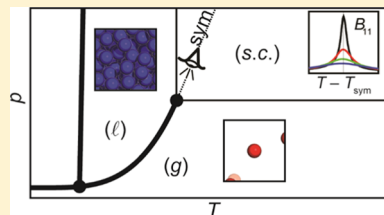
INTRODUCTION

"What are the fundamental characteristics of a gas or a liquid?" is a common question posed by many science teachers. The usual answers involve differences in density/volume or the ability to fill, or not fill, the container in which they are placed. These are perfectly satisfactory answers for most situations. However, phase diagrams of pure fluids indicate that as one increases the temperature (T) and/or pressure (p), there comes a point at which the distinction between a gas and a liquid disappears in the everyday sense. This marks the onset of the supercritical region. Consequently, supercritical fluids are neither gases nor liquids, and there is no phase transition in this region (see the excellent historical perspective by Levelt Sengers for further details[1]). Nevertheless, in the supercritical region, one does observe significant changes in fluid density over relatively small temperature ranges. These changes in density are expected to correlate with changes in other properties of interest. Hence, there remains a strong desire to attribute the properties of supercritical fluids to be either gas-like (low density) or liquid-like (high density),[1−4] due to the many potential and realized applications of supercritical fluids. This, in turn, requires that we answer the fundamental question: "What physical or thermodynamic metric can be used to unambiguously distinguish between a gas and a liquid?"

The behavior of common thermodynamic properties of pure fluids in the supercritical region, including the approach to the critical point, has been the subject of intense experimental and theoretical interest.[5−8] In particular, significant thought and effort have addressed the nature of the critical exponents that characterize the divergence of a range of thermodynamic properties at the critical point.[9,10] Although these studies are largely of theoretical interest, the study of supercritical fluids in the vicinity of the critical point is also a practical concern.

Solutes in supercritical fluids display a variety of interesting properties with promising applications as diverse as nuclear engineering, green chemistry, nanoparticle formation, and biomass remediation.[11−14] Furthermore, the petroleum industry uses supercritical fluids for upgrading high-molar-mass petroleum[15−18] and for petroleum demetallization,[19,20] gasification,[21,22] pyrolysis,[23] and chromatographic analysis.[24,25] However, before one can fully understand the behavior of specific solutes in supercritical fluids, one requires a full understanding of the pure fluids themselves. Consequently, there have been many attempts to assign gas-like or liquid-like behavior in the supercritical region of a fluid in an effort to understand their supercritical properties.[3,26−30]

Several properties have been used in previous attempts to divide the supercritical region into gas-like and liquid-like areas. These are summarized in Table 1. The first was the so-called "Widom line."[31−36] Although the exact origin is somewhat obscure,[26] it is now generally agreed to correspond to a maximum in the correlation length characterizing the range of the molecular interactions.[37] An alternative is provided by Nishikawa and co-workers, who have studied the behavior of density fluctuations in fluids.[39,41−46] The "Nishikawa line" or "ridge" is associated with a maximum in the structure factor along an isotherm.[47−49] Unfortunately, an experimental determination of the correlation length and/or structure factor requires scattering studies, and, in particular, it is not provided by typical equations of state (EOS) used to correlate fluid properties. Consequently, many studies have used the response functions as a substitute. It is most common to use the maximum in the isobaric heat capacity (C_P) along

Table 1. Lines Used to Distinguish Gas-like and Liquid-like Areas within the Supercritical Region

name of line	definitions used in the literature[a]
Frenkel line	State points for which the velocity autocorrelation function for the fluid changes from having the oscillatory behavior characteristic of liquids to the nonoscillatory behavior characteristic of gases.[38] Also located by the state points for which the constant volume molar heat capacity = $2k_B$.[38]
Nishikawa line or "ridge"	Maximum in $\langle(\delta N_1)^2\rangle/\langle N_1\rangle = S(0)$ wrt p along an isotherm.[39]
pseudocritical line	Maximum in C_p wrt T along an isobar.[13]
Widom line	Maximum in the correlation length.[37,38] Proxies: maximum in response functions (most often C_p, but also κ_T or α_p) wrt T along an isobar or, sometimes, wrt p along an isotherm.[4,37,40]
symmetry line	Maximum in $\langle(\delta N_1)^2\rangle/V = B_{11}$ wrt p along an isotherm.

[a]See the text for symbol definitions and additional references. Some definitions have changed over time, so only recent definitions/references were given.

each isobar (or, sometimes, isotherm)[4,37,50] to provide a reasonable indication of the Widom line. The maximum in C_p along an isobar is also known as the pseudocritical line.[13] However, there is no rigorous justification for this choice and therefore, in principle, any of the response functions could be used. Close to the critical point, the choice is relatively unimportant as all of the maxima closely coincide, but further from the critical point ($>\sim$20 K for water), the maxima in the response functions begin to deviate significantly from each other. A crossover in dynamical behavior in the supercritical region, sometimes referred to as the "Frenkel line," has also been observed.[4,27,37,38,40,51−55] This crossover appears to be correlated with the Widom line,[37] although it is primarily associated with the properties of the velocity autocorrelation, which are not directly available experimentally.[51] Furthermore, rather than being uniquely defined, it is obtained by noting the proximity of state points for multiple criteria.[27,52] Clearly, a more practical and easily accessible separation into gas-like and liquid-like regions is desirable.

In an effort to distinguish between gas- and liquid-like behavior in all fluid regions of the phase diagram, we have turned to Kirkwood−Buff (KB) theory, also known more generally as fluctuation solution theory (FST).[56−64] KB/FST is an exact statistical mechanical theory that can be used to study both liquids and gases.[56,62−65] KB theory provides relationships between either the pair distribution functions or the pair particle fluctuations and basic thermodynamic properties of the system. The extensions of the theory that we refer to as FST involve either the inclusion of higher-order fluctuations (triplet, etc.) and/or the inclusion of energy fluctuations, which removes the isothermal restriction.[58−61,66−69] It should be noted that FST assumes nothing concerning the nature or spatial range of the interactions.

When applied to a pure fluid, FST provides relationships between thermodynamic properties of a closed system at a particular pressure (p), temperature (T), and density (ρ_1) and the corresponding fluctuations observed for an equivalent system in the grand canonical ensemble (GCE).[57] FST has been used to study a variety of properties for pure fluids and liquid mixtures.[65] Most studies have focused on only the pair correlations in pure fluids. Indeed, the behavior of most properties as one approaches the critical point is well established.[5,70−73] Recently, we presented a discussion of the behavior of the pair, triplet, and quadruplet fluctuations

(including the associated distribution function integrals) covering a large segment of the water phase diagram using an accurate equation of state.[60] Here, we extend that analysis to include the supercritical region and the approach to the critical point (T_c, p_c, $\rho_{1,c}$) for multiple fluids. In particular, we identify crossover behavior characteristic of the gas and liquid regions in all pure fluids.

■ THEORY

The GCE properties of interest here are the particle number (N_1) or excess energy (ε) fluctuation densities given by the intensive quantities,[59,60]

$$B_{yz} \equiv \langle\delta y\delta z\rangle/V$$

$$C_{xyz} \equiv \langle\delta x\delta y\delta z\rangle/V$$

$$D_{wxyz} \equiv [\langle\delta w\delta x\delta y\delta z\rangle - \langle\delta w\delta x\rangle\langle\delta y\delta z\rangle - \langle\delta w\delta y\rangle\langle\delta x\delta z\rangle$$
$$- \langle\delta w\delta z\rangle\langle\delta x\delta y\rangle]/V$$

$$(1)$$

where $\delta z = z - \langle z\rangle$, etc., denotes a fluctuation in the value of $z = N_1$ or ε, V is the volume of the system, and the angular brackets denote a GCE average at the density ($\rho_1 = \langle N_1\rangle/V$) and temperature of interest. The excess energy is given by $\varepsilon \equiv E - N_1 H_1$, where E and N_1 are the instantaneous (in a time sense) internal energy and number of particles for the system, and H_1 is the average molar enthalpy of the pure fluid (1). Note that "1" will be used as a shorthand for "N_1" in the subscripts of B, C, and D. The above quantities were obtained by repeated differentiation of the GCE partition function with respect to the chemical potential,[60,70,72] and the choice of this particular form of excess energy is outlined elsewhere.[74] The pair (B's), triplet (C's), and quadruplet (D's) fluctuations can be related to integrals over the pair, triplet, and quadruplet spatial molecular correlation functions if desired.[60,75] The pair correlations can also be expressed in terms of a short-range direct correlation function using the Ornstein−Zernike equation.[5,72] However, neither of these extensions is required for the present analysis.

The application of FST to classical fluids provides relationships between common thermodynamic properties and the above fluctuating quantities. Hence, the fluctuations can easily be extracted from the relevant experimental data.[76] The pair particle fluctuations are given by,[57,72,74]

$$Z\frac{B_{11}}{\rho_1} = p\kappa_T$$

$$(2)$$

where $\kappa_T = \rho_1^{-1}(\partial\rho_1/\partial p)_T$ is the isothermal compressibility, $Z = \beta p/\rho_1$ is the compressibility factor, $\beta = (RT)^{-1}$, and R is the gas constant. The above expression corresponds to the compressibility equation,[72] which also characterizes the divergence of the particle number (density) fluctuations, $\langle\delta N_1\delta N_1\rangle = B_{11}V$, as one approaches the critical point. Also of primary concern will be the triplet particle number fluctuations, which are obtained after taking a pressure derivative of eq 2 to give,[60,76]

$$Z^2\frac{C_{111}}{\rho_1} = (p\kappa_T)^2 + \frac{p^2}{\rho_1}\frac{\partial^2\rho_1}{\partial p^2}$$

$$(3)$$

Alternatively, taking a temperature derivative of eq 2, one finds,[60,76]

$$Z \frac{\beta C_{11\varepsilon}}{\rho_1} = p\kappa_T (1 - T\alpha_p) + \frac{Tp}{\rho_1} \frac{\partial^2 \rho_1}{\partial T \partial p} \qquad (4)$$

where $\alpha_p = -\rho_1^{-1}(\partial \rho_1 / \partial T)_p$ is the thermal expansion coefficient. Finally, the pressure and temperature derivatives of eq 3 provide two quadruplet fluctuation densities,[60,76]

$$Z^3 \frac{D_{1111}}{\rho_1} = (p\kappa_T)^3 + 4p\kappa_T \frac{p^2}{\rho_1} \frac{\partial^2 \rho_1}{\partial p^2} + \frac{p^3}{\rho_1} \frac{\partial^3 \rho_1}{\partial p^3} \qquad (5)$$

$$Z^2 \frac{\beta D_{111\varepsilon}}{\rho_1} = T\alpha_p (p\kappa_T)^2 + 2p\kappa_T \frac{Tp}{\rho_1} \frac{\partial^2 \rho_1}{\partial T \partial p} + \frac{Tp^2}{\rho_1} \frac{\partial^3 \rho_1}{\partial T \partial p^2}$$
$$+ 2(1 - T\alpha_p)\left[(p\kappa_T)^2 + \frac{p^2}{\rho_1} \frac{\partial^2 \rho_1}{\partial p^2} \right] \qquad (6)$$

Other fluctuating quantities are also available,[76] but they are not required here. All pressure derivatives are isothermal and all temperature derivatives are isobaric in the above equations, and the required derivatives are generally available from an (accurate) EOS.[60] They can be applied to the gas, liquid, and solid phases away from a first-order phase transition. All properties described here were determined using the IAPWS-95 EOS for water,[77] Tegeler et al. EOS for argon,[78] Span and Wagner EOS for CO_2,[79] and Guder and Wagner EOS for SF_6.[80] More details can be found elsewhere.[60]

Clearly, eq 2 simply relates the fluid compressibility to a single fluctuating quantity for an equivalent GCE system, and, therefore, any additional insight into the behavior of fluids is relatively minor. However, eqs 3−6 relate fluctuating quantities to combinations of thermodynamic derivatives. Hence, it is possible to obtain new insights into fluid behavior not provided by the examination of the traditional thermodynamic derivatives themselves. Similar thermodynamic derivatives have been used by Koga and co-workers to study the properties of pure liquids and liquid mixtures.[81,82] However, these studies correspond to different derivatives than those considered here and have generally not involved the supercritical region.

■ RESULTS AND DISCUSSION

Triplet Particle Number Fluctuations can Distinguish between Gas and Liquid Behavior in all Fluid Regions of the Phase Diagram. The results from an FST analysis of the particle number fluctuations for fluid water are presented in Figure 1, and a more complete analysis is provided elsewhere.[76] The $p-T$ plane is displayed here due to the extensive use of isothermal pressure derivatives in eqs 2, 3, and 5. As expected, B_{11} increases dramatically as one approaches the critical point. The fluctuation densities exhibit maxima or minima in the supercritical region, along an isotherm and/or isobar, and C_{111} and D_{1111} change signs in this region. The behavior of C_{111} is most notable. It is clear that C_{111} is always negative in the liquid region and always positive in the gas region. Furthermore, this behavior extends beyond the liquid−gas line with the triplet fluctuations changing sign in the supercritical region. Identical behavior is observed in a previous FST analysis of CO_2 and SF_6[76] and is also illustrated in Figure 2 for these fluids as well as argon. Clearly, the phase dependence for the sign of C_{111} is a general result.

The above fluctuations correspond to the cumulants of the particle number and/or excess energy distribution for the
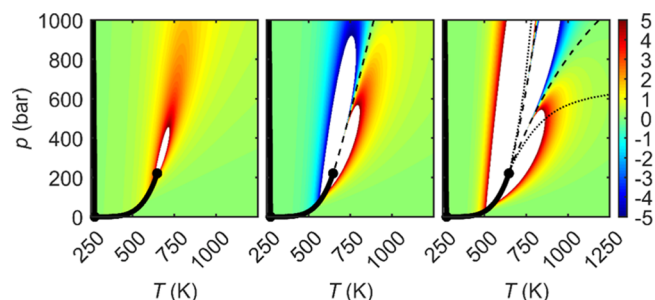

Figure 1. Left to right: Dimensionless pair ($B_{11}/\rho_{1,c}$), triplet ($C_{111}/\rho_{1,c}$), and quadruplet ($D_{1111}/\rho_{1,c}$) particle number fluctuation densities for the liquid, gas, and supercritical region of water as a function of pressure and temperature. The thick black curves correspond to the phase boundaries, whereas the triple point ($p_{tp} = 0.006$ bar, $T_{tp} = 273.16$ K) and critical point ($p_c = 220.64$ bar, $T_c = 647.10$ K, and $\rho_{1,c} = 17.874$ mol/L) are denoted by black circles. The state points for which the property is equal to zero (not applicable to $B_{11}/\rho_{1,c}$) are marked with dashed curves. The state points that correspond to the higher- and lower-pressure maxima in D_{1111} are shown as dotted curves in the third column.
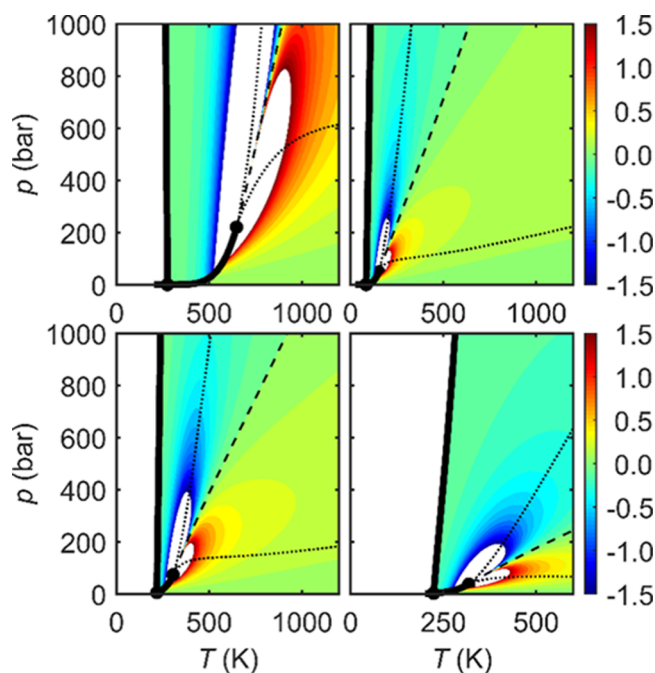

Figure 2. Dimensionless triplet particle number fluctuations ($C_{111}/\rho_{1,c}$) for the liquid, gas, and supercritical regions of H_2O (top left), argon (top right), CO_2 (bottom left), and SF_6 (bottom right) as a function of pressure and temperature. The dashed curves correspond to $C_{111} = 0$. The dotted curves correspond to the higher- and lower-pressure maxima in D_{1111}. Tabulated values of p, T, and ρ_1 along the symmetry line and the max(D_{1111}) curves for all four systems are provided in the Supporting Information.

equivalent open system[70] that can be interpreted using standard statistical approaches.[83] Focusing on the particle number distribution, we find that B_{11} provides the variance of the particle number distribution for a unit volume of the fluid. The values C_{111} and D_{1111} provide the corresponding skewness and excess kurtosis of the distribution in terms of the central moments.[83] A Gaussian or normal particle number distribution corresponds to $C_{111} = D_{1111} = 0$, whereas symmetric distributions require at least $C_{111} = 0$, i.e., zero skewness. If

C_{111} is positive, then particle addition (in the GCE) is more probable than removal at a particular state point or vice versa, whereas a positive value for D_{1111} indicates that the distribution is more peaked than that of a normal distribution with the same variance. Figure 1 shows that the particle number distribution is not Gaussian for a real fluid at any state point.[74] Indeed, the triplet fluctuations quantified by C_{111} are always positive in the gas phase ($B_{11} = C_{111} = \rho_1$ for an ideal gas) and always negative in the liquid phase.[60] Hence, particle addition is more probable than removal for gases, whereas particle removal is more probable than addition in liquids, presumably due to the higher particle densities involved. Consequently, it seems logical to use C_{111}, which has a clear physical interpretation, to separate supercritical behavior into gas-like and liquid-like regions.

Equation 2 provides only minor additional insight into the behavior of fluids, since it relates κ_T to a single fluctuating quantity for an equivalent GCE system. However, as mentioned previously, eqs 3−6 relate fluctuating quantities to combinations of thermodynamic derivatives, providing new insights into fluid behavior not provided by the examination of the traditional thermodynamic derivatives themselves. Notably, FST can be used to provide an unambiguous dividing line (strictly a curve) between gas-like (disordered state) and liquid-like (ordered state) behavior that extends into the supercritical region without the need for scattering experiments. In the supercritical region, the dividing line corresponds to state points for which $C_{111} = 0$ and infers a degree of symmetry (zero skewness) displayed by the particle number distribution for the equivalent GCE system. We will henceforth refer to this line as the *symmetry line*. The symmetry line can be considered "hidden" in a sense, because it corresponds to a combination of traditional thermodynamic properties (see eq 3). This symmetry line is not to be confused with the line of symmetry proposed in a previous analysis by Widom and Stillinger.[84] The present work does not make use of statistical field theories. Thus, our use of the word "symmetry" is not meant to presuppose the imposition of symmetry or, in contrast, the use of an asymmetric correction in the construction of an effective Hamiltonian in the statistical field theory.[85−91]

The symmetry line corresponds to a maximum in the pair particle number fluctuation density with respect to pressure along an isotherm, as given by the relationship,[59]

$$\left(\frac{\partial B_{11}}{\partial p}\right)_T = \beta \frac{C_{111}}{\rho_1} \tag{7}$$

This is also equivalent to a maximum in $\rho_1^2 RT \kappa_T$ along an isotherm or to a maximum in the susceptibility, $\chi = (\partial \rho_1/\partial \mu_1)_T = \rho_1^2 \kappa_T$, along an isotherm, where the order parameter is the density and the chemical potential μ_1 is the field.[92] "Above" (lower T, higher p) this line, $C_{111} < 0$, and the supercritical fluid displays liquid-like behavior. "Below" (higher T, lower p) this line, $C_{111} > 0$, and the supercritical fluid displays gas-like behavior. It can be shown that the symmetry line also suggests that the characteristic thermodynamic difference between gases and liquids is that $(\partial^2 \rho_1/\partial \mu_1^2)_T > 0$ for gases and $(\partial^2 \rho_1/\partial \mu_1^2)_T < 0$ for liquids, whereas $(\partial^2 \rho_1/\partial \mu_1^2)_T = 0$ along the symmetry line. Other criteria exist and are provided in the Supporting Information. The symmetry lines for supercritical H_2O, Ar, CO_2, and SF_6 are displayed in Figure 2 in the $p−T$ plane.

Numerical values and figures in the $T−\rho_1$ and $p−\rho_1$ planes are provided in the Supporting Information.

The Symmetry Line Is Different from Other Measures of Gas-like and Liquid-like Transitions. The symmetry line is compared to the corresponding maxima for several other fluid properties in Figure 3. The symmetry line is most similar
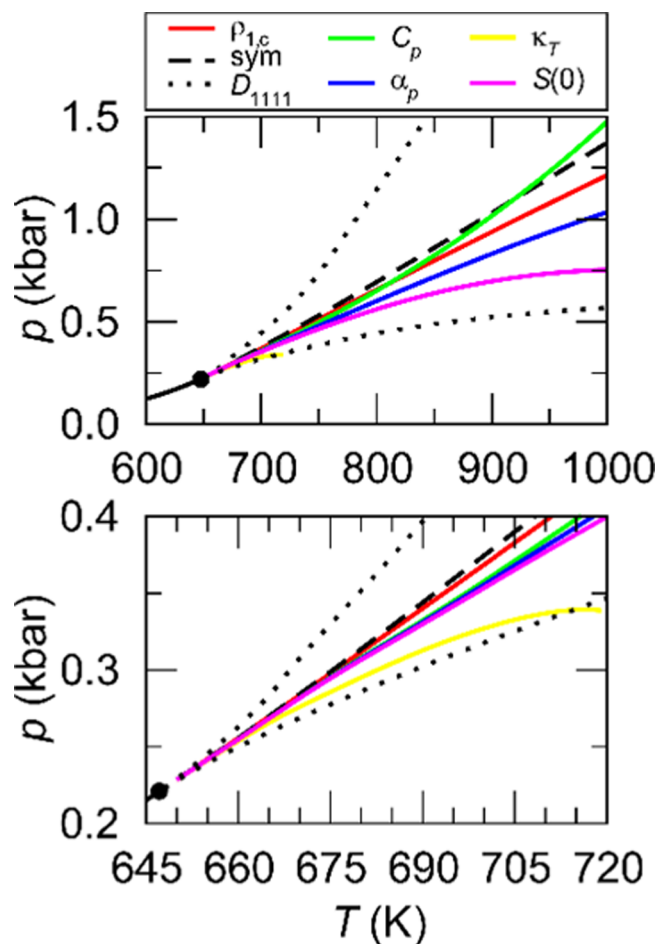

Figure 3. Location of the symmetry line compared to the critical isochore and other response functions for the supercritical region of water as a function of pressure and temperature far away from (top) and closer to the critical point (bottom). The symmetry line (dashed) is defined by $C_{111} = 0$, which also corresponds to a maximum in B_{11} as a function of pressure for each isotherm. The dotted curves correspond to the higher- and lower-pressure maxima in D_{1111}. The gas−liquid co-existence curve is displayed in the bottom left corner and ends at the critical point (denoted by the filled circle). Also displayed are the points for which the isobaric heat capacity, thermal expansion, compressibility, and structure factor are a maximum as a function of pressure along each isotherm. The maximum in the compressibility disappears beyond $\approx$ 720 K.

to the C_p-based proxy for the Widom line, but it is also clearly different. The symmetry line represents a simple extension of the liquid−vapor line into the supercritical region. Hence, the approach along the symmetry line from the supercritical region toward the critical point signals the crossover from liquid-like to gas-like behavior. In the supercritical region, this crossover can occur smoothly. However, in the subcritical region, the crossover results in a first-order phase transition with a discontinuous change in ρ_1 (and, therefore B_{11} and C_{111}) between the two separate phases. We note that the symmetry

line does not correspond to the critical isochore (for real fluids), the Widom line, the Nishikawa line, or the Frenkel line.[28] The Widom line corresponds to a maximum in the correlation length for a pure fluid. A reasonable proxy for this is provided by the (long wavelength) behavior of the fluid structural factor, $S(0)$.[5] This thermodynamic quantity is given by $S(0) = \rho_1 RT\kappa_T = B_{11}/\rho_1$ and is also shown in Figure 3. Using this proxy, a maximum in the structure factor along an isotherm corresponds to both the Widom and the Nishikawa lines.

To illustrate the above behavior in more detail, the nature of the fluctuating quantities perpendicular to the symmetry line has been examined as one proceeds from the liquid-like region, across the symmetry line, to the gas-like region. This is achieved by noting that the tangent to the symmetry line can be obtained from the differential of $C_{111}(p,T)$, which is always zero along the symmetry line, to give,[76]

$$\left(\frac{\partial p}{\partial T}\right)_{sym} = -\left(\frac{\partial C_{111}}{\partial T}\right)_p \left(\frac{\partial C_{111}}{\partial p}\right)_T^{-1} = -\frac{\rho_1}{T}\frac{D_{111\varepsilon}}{D_{1111}} \quad (8)$$

This also provides the slope of the line perpendicular to the tangent. The results are displayed in Figure 4 for temperatures along the symmetry line that lies close to the critical temperature. The data strongly suggest that as one approaches the critical point along the symmetry line, B_{11} tends to large
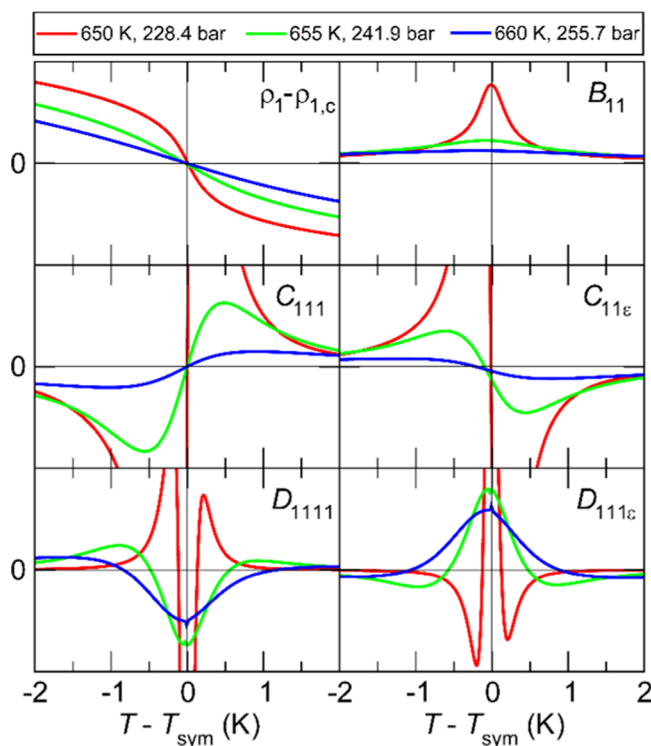

Figure 4. Density and fluctuation densities for water as a function of distance perpendicular to the symmetry line in the supercritical region close to the critical point. The symmetry line corresponds to $T - T_{sym} = 0$ along the line given by $p - p_{sym} = m_p (T - T_{sym})$, where $m_p = -(\partial T/\partial p)_{sym}$ is given by eq 8. Therefore, $T - T_{sym} < 0$ points lie in the liquid-like region, whereas $T - T_{sym} > 0$ points lie in the gas-like region. The colored curves correspond to different values of T_{sym} and p_{sym}, as denoted in the legend. The curves in each panel were arbitrarily scaled in the y-direction to emphasize the underlying features.

positive values (although not a maximum along the perpendicular line), C_{111} is zero (as expected), $C_{11\varepsilon}$ tends to zero, whereas D_{1111} and $D_{111\varepsilon}$ display large negative minima and positive maxima, respectively. The changes in the sign become more abrupt but still continuous, as one approaches the critical point. This is consistent with a symmetric particle number distribution where all of the odd cumulants are zero but whose width with respect to a Gaussian with the same variance is increasing dramatically. Eventually, the width of the distribution, and hence the fluctuations, becomes so large that the system separates to form both low- and high-density phases.

The corresponding behavior in the density, B_{11}, and the thermodynamic response functions perpendicular to the symmetry line are shown in Figure 5. Figure 5 also indicates
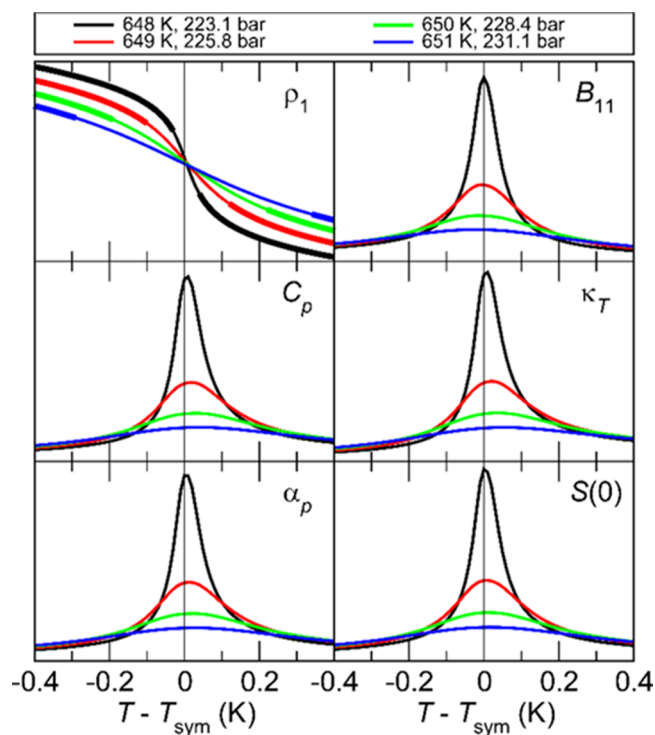

Figure 5. Density, B_{11}, and response functions for water as a function of distance perpendicular to the symmetry line in the supercritical region close to the critical point. All y-axis values are positive. The colored curves correspond to different values of T_{sym} and p_{sym}, as denoted in the legend. In the top left panel, the state points outside the transition region are shown in the thick line style, whereas the state points within the transition region are shown in the thinner line style. This designation of state points within and outside of the transition region applies to each panel, but it was only shown in the top left panel for clarity.

that there is a transition region bounding the changes in ρ_1 and the response functions perpendicular to the symmetry line. Away from the critical point, the transition region is rather broad. The properties of supercritical fluids will, therefore, change rather slowly in these regions. However, closer to the critical point, properties change more dramatically. The maxima in the thermodynamic response functions all show small deviations from the symmetry line, as also shown in Figure 3. This deviation decreases as one approaches the critical point.

Higher-Order Fluctuations Indicate a Transition Region between Pure Liquid and Pure Gas Behavior. The assignment of gas-like or liquid-like behavior for a fluid can be extended beyond the symmetry line to define a *transition region* where the properties of the fluid slowly change from that characteristic of a liquid to that characteristic of a gas or vice versa. We define the transition region to lie between the two pressures for which D_{1111} is a maximum along a particular isotherm. As shown in Figure 1, the sign of D_{1111} is always positive for both liquids and gases outside the supercritical region. However, within the supercritical region, D_{1111} becomes negative. This behavior indicates a transition region where a fluid moves from pure liquid properties ($C_{111} < 0$, $D_{1111} > 0$) to pure gas properties ($C_{111} > 0$, $D_{1111} > 0$). This may result in unique applications at these state points. An alternative definition for the transition region could have been to simply choose the region in which D_{1111} was negative, which would have resulted in a narrower transition region where either $C_{111} < 0$ and $D_{1111} < 0$ or $C_{111} > 0$ and $D_{1111} < 0$, i.e., where the fluid exists in a region in which the cumulants through fourth order are fundamentally different from those of a gas or a liquid. However, the definition of the transition region chosen ensures that the next cumulant, given by the isothermal pressure derivative of D_{1111}, will have the same sign outside the transition region (but within the supercritical region), as it does in the liquid and gas regions.

The transition region is also indicated in Figures 2, 3, and 5 in the $p-T$ plane and in Figures S1 and S2 for other planes. Figure 3 indicates that the maximum in the structure factor and the thermodynamic response functions fall within the transition region, except for the isothermal compressibility at high temperatures. Figure 5 indicates the transition region and how it relates to changes in the density and response functions perpendicular to the symmetry line. The transition region suggested here highlights state points between which the response functions display significant changes in their values.

Behavior of the Symmetry Line Close to the Critical Point. The behavior of the fluctuations along the symmetry line appears to be clear, even for states close to the critical point, as illustrated in Figure 4. However, the behavior at the critical point is not so conclusive for several reasons. First, an EOS has been used for the present analysis and therefore the observed behavior close to the critical point may be influenced by the properties of the EOS and not necessarily reflect the raw experimental data.[77,92] Hence, the present analysis has not included temperatures very close (mK) to the critical point. Nevertheless, the results are consistent between a variety of systems (H_2O, Ar, CO_2, and SF_6) and for a total of 12 accurate EOSs representing these four systems (data not shown). Second, the exact location of the symmetry line becomes more difficult to determine as the critical point is approached, primarily as one is attempting to find the maximum of a diverging property, B_{11}. Third, away from the symmetry line, C_{111} may only be exactly zero at the critical point. Adopting any other approach, along the critical isotherm, isobar, or isochore, C_{111} will appear to diverge to $\pm\infty$, as indicated in Figures 1 and 4 and our previous work.[60] Finally, the fluid properties may be influenced by surface effects close to the critical point.[93] Consequently, many of the thermodynamic relationships adopted here are then incorrect as they are based on Euler's theorem, which is no longer valid.[94,95] However, this would be true for any thermodynamic and/or statistical mechanical analyses of the experimental data.

As the critical point corresponds to an infinitesimally small region of the phase diagram, one can consider this point to be either the last point displaying a discontinuous transition between liquid and vapor, i.e., the last point along the liquid–vapor line, as T increases, or one can think of it as the first point after that, i.e., the last point along the symmetry line, as T is decreasing. The difference is essentially philosophical, because no experiment could distinguish between these two options as they differ by an infinitesimally small T (or p). In the former case, B_{11} would be discontinuous and diverging to infinity (although it is possible that this is only truly infinite for an infinite system). In the latter case, B_{11} would be (exceedingly) large but still display continuous derivatives.

Consequently, if one assumes or asserts that the particle number fluctuations tend to a finite maximum (for a very large but finite system size), then one can continue with this type of approach and investigate the consequences. Under these conditions, the pressure and temperature derivatives of B_{11} at the critical point are provided by the relationships,[60]

$$\left(\frac{\partial B_{11}}{\partial p}\right)_{T_c} = \frac{C_{111}}{\rho_{1,c} R T_c}$$

$$\left(\frac{\partial B_{11}}{\partial T}\right)_{p_c} = \frac{C_{11\varepsilon}}{R T_c^2}$$

$$\left(\frac{\partial B_{11}}{\partial T}\right)_{\rho_{1,c}} = \frac{C_{11\varepsilon}}{R T_c^2} + \frac{C_{111}}{\rho_{1,c} R T_c}\left(\frac{\partial p}{\partial T}\right)_{\rho_{1,c}}$$

$$\left(\frac{\partial B_{11}}{\partial T}\right)_{sym} = \frac{C_{11\varepsilon}}{R T_c^2} \tag{9}$$

where all fluctuating quantities correspond to the values at the critical point. The relationships in eq 9 were obtained from the differentials of $B_{11}(\beta\mu_1,\beta)$ or $B_{11}(p,\beta)$.[60,76] This is characteristic of a point maximum in the $p-T$ phase diagram with analytic derivatives. Hence, the pair fluctuations are increasing rapidly at the expense of the triplet fluctuations, as one approaches the critical point along the symmetry line. This is characteristic of mean field behavior but with the additional observation that as $C_{11\varepsilon} = C_{11E} - C_{111}H_1$, the energy and particle number correlation is zero, i.e., $C_{11E} = 0$, at the critical point. Furthermore, the above equations strongly suggest that the critical isochore, isobar, isotherm and the symmetry line then intersect at the critical point. Unfortunately, for Ising-type behavior, the above derivatives are undefined at the critical point.

Symmetry Line is Unique. Obviously, as mentioned previously, there have been many attempts to delineate liquid and gas behavior in the supercritical region. We have focused on the behavior of the particle number fluctuation density, B_{11}. Although it might not be possible to make a definitive choice among all of the alternatives, there are multiple arguments for adopting this particular quantity. First, B_{11} is most closely related to the density fluctuations that characterize the approach to the critical point and give rise to critical opalescence. Indeed, in a recent publication, we showed how the dominance of the particle number fluctuations (over the energy fluctuations) allows one to quantitatively predict the ratios of many of the diverging response functions at the critical point.[96] More important, however, is the fact that the corresponding triplet fluctuations, C_{111}, given by a simple

isothermal pressure derivative of B_{11} (see eq 7) adopt different signs for the whole of the liquid and gas regions. Second, the sign of C_{111} has a physical interpretation in terms of the ease of particle insertion or removal, with gases favoring particle insertion and liquids favoring particle removal. Third, although there are many possible closely related quantities to B_{11} that could serve as a transition line, B_{11} itself appears to be the simplest and most appropriate. Fisher and co-workers have investigated the behavior of a series of k-susceptibility loci, corresponding to the isothermal maxima of the corresponding susceptibilities, as one approaches the critical point. These are given by $B_{11}/\rho_1{}^k$ in our notation.[97,98] The symmetry line corresponds to $k = 0$, whereas $k = 1$ and 2 correspond to $S(0)$, related to the Nishikawa line, and κ_T, respectfully. However, although the symmetry line extends indefinitely within the supercritical region, the maximum in the $k = 1$ and 2 susceptibilities (and presumably $k > 2$) either vanishes or tends to ideal gas behavior for large T. Hence, it appears that they cannot be used to uniquely characterize gas and/or liquid behavior. Furthermore, the pressure maxima in the above susceptibilities along an isotherm correspond to the condition $\rho_1 C_{111} = k\,B_{11}{}^2$.[60,97,98] This is incompatible with the observed behavior of C_{111}, namely, negative for liquids and positive for gases, as the maxima would have to appear in the gas phase for all but $k = 0$. Alternatively, Woodcock has focused on the behavior of the derivative $(\partial p/\partial\rho_1)_T \equiv \omega$, termed the fluid "rigidity."[3] Woodcock has inferred a mesophase, corresponding to regions of constant rigidity, which is bounded by gas and liquid behavior.[3,29,30] The symmetry line corresponds to a maximum in $1/\omega$, whereas the transition region presented here is qualitatively similar to the mesophase presented by Woodcock. Fourth, the examination of higher cumulants of the particle number density distribution provides for the definition of a transition region, as described earlier. Finally, other efforts that follow the maximum in a thermodynamic response function have a variety of available properties to select from as well as a few choices for which maximum to take (along an isotherm, isobar, or isochore). There appears to be no definitive underlying theoretical (statistical mechanical or otherwise) guidance for these choices. In contrast, C_{111}, which represents a nonobvious combination of thermodynamic derivatives, naturally emerges from the FST statistical mechanical treatment of pure fluids.

Statistical mechanics allows us to use any convenient ensemble to study the average properties of systems as these are independent of the ensemble. Fluctuations, however, are ensemble-dependent, and, in particular, the particle number fluctuations adopted here appear specific to the GCE. Fortunately, as we have recently shown,[74] the pair and triplet fluctuations in different ensembles are related to the same thermodynamic derivatives in a simple manner. For instance, the isothermal compressibility in the GCE is given by eq 2. This can be converted to the corresponding expression in the NpT ensemble by the transformation $\delta N_1 \rightarrow -\rho_1\delta V$. Hence, all of the observations concerning the particle number fluctuations in the previous sections also refer to the volume fluctuations in the NpT ensemble. Even the sign change can be rationalized by consideration of the density for which we have $\delta\rho_1/\rho_1 = \delta N_1/N_1 - \delta V/V$. Consequently, the above behavior fits nicely into the concept of free volume that was used in early attempts to distinguish the states of matter[2,99−101] and more recent studies invoking percolation transitions.[3,29,30,36] We also note that the particle number fluctuations are directly related to fluctuations in the Gibbs free energy ($G = \mu_1 N_1$) as $\delta G = \mu_1\,\delta N_1$ for a pure fluid in the GCE. On the other hand, C_p is related to the pair enthalpy (or entropy) fluctuations in the NpT ensemble and to the excess energy fluctuations in the GCE. However, isothermal pressure derivatives of C_p do not provide the corresponding triplet fluctuations but rather a mixed enthalpy−enthalpy−volume fluctuation. The behavior of the pure triplet enthalpy fluctuations could be obtained and investigated via isobaric temperature derivatives of T^2C_p. Unfortunately, our preliminary investigations in this direction indicate that these derivatives do not exhibit characteristic signs in the gas and liquid regions. These observations suggest that the particle number fluctuations are unique in their behavior and provide a general picture of the fluid thermodynamics.

■ CONCLUSIONS

An FST analysis of a range of fluids suggests that the particle number (density) distribution for any pure classical fluid has a positive skewness in the gas phase and a negative skewness in the liquid phase. This appears to be the property that characteristically distinguishes gases from liquids, thus answering the question posed at the beginning of the article for any pure classical fluid. Physically, this implies that particle addition is more favorable than removal for gases, leading to a bias toward higher density fluctuations, whereas particle removal is more favorable than addition for liquids, leading to a bias toward lower density fluctuations. The supercritical region of all fluids contains a line (technically a curve) where the skewness is zero. This "symmetry line" joins the liquid−vapor co-existence curve at the critical point. Consequently, liquid-like and gas-like behavior (through third order) can be inferred by the sign of the cumulants characterizing the particle number distribution and can be used to help rationalize the properties of supercritical fluids. Because the symmetry line is obtained by a combination of thermodynamic properties, it is, in a sense, "hidden."

By considering the next cumulant (excess kurtosis), a "transition region" surrounding the symmetry line can be observed, within which the fluctuations through fourth-order change from that characteristic of a pure liquid (negative skewness and positive excess kurtosis) to that characteristic of a pure gas (where the skewness and excess kurtosis are both positive) or vice versa. This is only possible by the use of a statistical mechanical approach, as outlined here.

The consequences for the nature of the approach to the critical point from the supercritical region are also potentially interesting. If the critical point is considered to be the last state point along the symmetry line for which continuous derivatives of B_{11} are obtained, then B_{11} is a maximum and C_{111} is zero at the critical point. This is consistent with the mean field behavior. Unfortunately, for any approach other than along the symmetry line, i.e., along the critical isochore, isotherm, or isobar, the value of C_{111} will appear to diverge to $\pm\infty$, suggesting that no continuous maximum exists for B_{11}. It is possible, therefore, that the approach along the critical isochore exhibits Ising-type behavior, whereas the approach along the symmetry line exhibits mean field behavior. Furthermore, as it becomes increasingly more difficult to distinguish between the symmetry line and the critical isochore close to the critical point (they meet tangentially) it is also possible to observe a crossover from mean field to Ising

behavior, or vice versa, depending on the exact experimental conditions, as observed experimentally.[102−104]

■ ASSOCIATED CONTENT

ⓢ Supporting Information

The Supporting Information is available free of charge on the ACS Publications website at DOI: 10.1021/acs.jpcb.9b04058.

> Alternative ($\rho_1 - T$ and $\rho_1 - p$) phase diagrams showing the symmetry and max(D_{1111}) state points (Figures S1 and S2); symmetry curve and upper- and lower-pressure max(D_{1111}) curves for select state points (Tables S1−S4) (PDF)

■ AUTHOR INFORMATION

Corresponding Author

*E-mail: pesmith@ksu.edu.

ORCID ⓞ

Paul E. Smith: 0000-0002-5565-3274

Author Contributions

The manuscript was written through contributions of all authors.

Notes

The authors declare no competing financial interest.

■ ACKNOWLEDGMENTS

■ ABBREVIATIONS

EOS, equation of state; FST, fluctuation solution theory; GCE, grand canonical ensemble; KB, Kirkwood−Buff

■ REFERENCES

(1) Levelt Sengers, J. M. H. Liquidons and gasons; controversies about the continuity of states. *Phys. A* **1979**, *98*, 363−402.

(2) Frenkel, J. I. *Kinetic Theory of Liquids*. Unabridged and unalt. repub. ed.; Dover Publications: New York, 1955.

(3) Woodcock, L. V. Thermodynamics of gas−liquid criticality: Rigidity symmetry on Gibbs density surface. *Int. J. Thermophys.* **2016**, *37*, 24.

(4) Simeoni, G. G.; Bryk, T.; Gorelli, F. A.; Krisch, M.; Ruocco, G.; Santoro, M.; Scopigno, T. The Widom line as the crossover between liquid-like and gas-like behaviour in supercritical fluids. *Nat. Phys.* **2010**, *6*, 503−507.

(5) Stanley, H. E. *Introduction to Phase Transitions and Critical Phenomena*; Oxford University Press: New York, 1971.

(6) Domb, C. *The Critical Point: A Historical Introduction to the Modern Theory of Critical Phenomena*; Taylor & Francis Ltd: London, 1996.

(7) Anisimov, M. A. *Critical Phenomena in Liquids and Liquid Crystals*; Gordon & Breach Science: New York, 1991.

(8) Lesne, A. *Renormalization Methods: Critical Phenomena, Chaos, Fractal Structures*; John Wiley & Sons Ltd: Chichester, 1995.

(9) Sengers, J. V.; Shanks, J. G. Experimental critical-exponent values for fluids. *J. Stat. Phys.* **2009**, *137*, 857−877.

(10) Anisimov, M. A. Letter to the editor: Fifty years of breakthrough discoveries in fluid criticality. *Int. J. Thermophys.* **2011**, *32*, 2001−2009.

(11) Brunner, G. Applications of supercritical fluids. *Annu. Rev. Chem. Biomol. Eng.* **2010**, *1*, 321−342.

(12) Cansell, F.; Aymonier, C.; Loppinet-Serani, A. Review on materials science and supercritical fluids. *Curr. Opin. Solid State Mater. Sci.* **2003**, *7*, 331−340.

(13) Pioro, I.; Mokry, S.; Draper, S. Specifics of thermophysical properties and forced-convective heat transfer at critical and supercritical pressures. *Rev. Chem. Eng.* **2011**, *27*, 191−214.

(14) Mathias, P. M.; Copeman, T. W.; Prausnitz, J. M. Phase equilibria for supercritical extraction of lemon flavors and palm oils with carbon dioxide. *Fluid Phase Equilib.* **1986**, *29*, 545−554.

(15) Shu, D.; Chi, Y.; Liu, J.; Huang, Q. Characterization of water-in-oil emulsion and upgrading of asphalt with supercritical water treatment. *Energy Fuels* **2017**, *31*, 1468−1477.

(16) Dimitrelis, D.; Prausnitz, J. M. Solubilities of n-octadecane, phenanthrene, and n-octadecane/phenanthrene mixtures in super-critical propane at 390 and 420 K and pressures to 60 bar. *J. Chem. Eng. Data* **1989**, *34*, 286−291.

(17) Radosz, M.; Cotterman, R. L.; Prausnitz, J. M. Phase equilibria in supercritical propane systems for separation of continuous oil mixtures. *Ind. Eng. Chem. Res.* **1987**, *26*, 731−737.

(18) Kim, D.-W.; Ma, F.; Koriakin, A.; Jeong, S.-Y.; Lee, C.-H. Parametric study for upgrading petroleum vacuum residue using supercritical m-xylene and n-dodecane solvents. *Energy Fuels* **2015**, *29*, 2319−2328.

(19) Jenifer, A. C.; Sharon, P.; Prakash, A.; Sande, P. C. A review of the unconventional methods used for the demetallization of petroleum fractions over the past decade. *Energy Fuels* **2015**, *29*, 7743−7752.

(20) Magomedov, R. N.; Pripakhaylo, A. V.; Maryutina, T. A. Solvent demetallization of heavy petroleum feedstock using super-critical carbon dioxide with modifiers. *J. Supercrit. Fluids* **2017**, *119*, 150−158.

(21) Qian, Y.; Yang, Q.; Zhang, J.; Zhou, H.; Yang, S. Development of an integrated oil shale refinery process with coal gasification for hydrogen production. *Ind. Eng. Chem. Res.* **2014**, *53*, 19970−19978.

(22) Susanti, R. F.; Dianningrum, L. W.; Yum, T.; Kim, Y.; Lee, Y.-W.; Kim, J. High-yield hydrogen production by supercritical water gasification of various feedstocks: Alcohols, glucose, glycerol and long-chain alkanes. *Chem. Eng. Res. Des.* **2014**, *92*, 1834−1844.

(23) DeWitt, M. J.; Edwards, T.; Shafer, L.; Brooks, D.; Striebich, R.; Bagley, S. P.; Wornat, M. J. Effect of aviation fuel type on pyrolytic reactivity and deposition propensity under supercritical conditions. *Ind. Eng. Chem. Res.* **2011**, *50*, 10434−10451.

(24) Lundanes, E.; Iversen, B.; Greibrokk, T. Group separation of petroleum using supercritical fluids. *J. Chromatogr. A* **1986**, *366*, 391−395.

(25) Qian, K.; Di Sanzo, F. P. Detailed analysis of olefins in processed petroleum streams by combined multi-dimensional super-critical fluid chromatography and field ionization Time-of-Flight Mass Spectrometry. *Energy Fuels* **2016**, *30*, 98−103.

(26) Fisher, M. E.; Widom, B. Decay of correlations in linear systems. *J. Chem. Phys.* **1969**, *50*, 3756−3772.

(27) Brazhkin, V. V.; Fomin, Y. D.; Lyapin, A. G.; Ryzhov, V. N.; Trachenko, K. Two liquid states of matter: A dynamic line on a phase diagram. *Phys. Rev. E* **2012**, *85*, No. 031203.

(28) Gorelli, F. A.; Bryk, T.; Krisch, M.; Ruocco, G.; Santoro, M.; Scopigno, T. Dynamics and thermodynamics beyond the critical point. *Sci. Rep.* **2013**, *3*, No. 1203.

(29) Heyes, D. M.; Woodcock, L. V. Critical and supercritical properties of Lennard-Jones fluids. *Fluid Phase Equilib.* **2013**, *356*, 301−308.

(30) Woodcock, L. V. Observations of a thermodynamic liquid−gas critical coexistence line and supercritical fluid phase bounds from percolation transition loci. *Fluid Phase Equilib.* **2013**, *351*, 25−33.

(31) McMillan, P. F.; Stanley, H. E. Going supercritical. *Nat. Phys.* **2010**, *6*, 479−480.

(32) Luo, J.; Xu, L.; Lascaris, E.; Stanley, H. E.; Buldyrev, S. V. Behavior of the Widom line in critical phenomena. *Phys. Rev. Lett.* **2014**, *112*, No. 135701.

(33) Raju, M.; Banuti, D. T.; Ma, P. C.; Ihme, M. Widom lines in binary mixtures of supercritical fluids. *Sci. Rep.* **2017**, *7*, No. 3027.

(34) Pipich, V.; Schwahn, D. Densification of supercritical carbon dioxide accompanied by droplet formation when passing the Widom line. *Phys. Rev. Lett.* **2018**, *120*, No. 145701.

(35) Śmiechowski, M.; Schran, C.; Forbert, H.; Marx, D. Correlated particle motion and THz spectral response of supercritical water. *Phys. Rev. Lett.* **2016**, *116*, No. 027801.

(36) Strong, S. E.; Shi, L.; Skinner, J. L. Percolation in supercritical water: Do the Widom and percolation lines coincide? *J. Chem. Phys.* **2018**, *149*, No. 084504.

(37) Xu, L. M.; Kumar, P.; Buldyrev, S. V.; Chen, S. H.; Poole, P. H.; Sciortino, F.; Stanley, H. E. Relation between the Widom line and the dynamic crossover in systems with a liquid-liquid phase transition. *Proc. Natl. Acad. Sci. U.S.A.* **2005**, *102*, 16558−16562.

(38) Prescher, C.; Fomin, Y. D.; Prakapenka, V. B.; Stefanski, J.; Trachenko, K.; Brazhkin, V. V. Experimental evidence of the Frenkel line in supercritical neon. *Phys. Rev. B* **2017**, *95*, No. 134114.

(39) Shibuta, S.; Imamura, H.; Nishikawa, K.; Morita, T. Fluctuational parameters based on the Bhatia−Thornton theory for supercritical solutions: Application to a supercritical aqueous solution of n-pentane. *Chem. Phys.* **2017**, *487*, 30−36.

(40) Gallo, P.; Corradini, D.; Rovere, M. Widom line and dynamical crossovers as routes to understand supercritical water. *Nat. Commun.* **2014**, *5*, No. 5806.

(41) Arai, A. A.; Morita, T.; Nishikawa, K. Investigation of structural fluctuation of supercritical benzene by Small-Angle X-ray Scattering. *J. Chem. Phys.* **2003**, *119*, 1502−1509.

(42) Morita, T.; Nishikawa, K.; Takematsu, M.; Iida, H.; Furutaka, S. Structure study of supercritical CO_2 near higher-order phase transition line by X-ray diffraction. *J. Phys. Chem. B* **1997**, *101*, 7158−7162.

(43) Nishikawa, K.; Morita, T. Inhomogeneity of molecular distribution in supercritical fluids. *Chem. Phys. Lett.* **2000**, *316*, 238−242.

(44) Nishikawa, K.; Tanaka, I. Correlation lengths and density fluctuations in supercritical states of carbon dioxide. *Chem. Phys. Lett.* **1995**, *244*, 149−152.

(45) Nishikawa, K.; Tanaka, I.; Amemiya, Y. Small-Angle X-ray Scattering study of supercritical carbon dioxide. *J. Phys. Chem. A* **1996**, *100*, 418−421.

(46) Saitow, K.-I.; Kajiya, D.; Nishikawa, K. Dynamics of density fluctuation of supercritical fluid mapped on phase diagram. *J. Am. Chem. Soc.* **2004**, *126*, 422−423.

(47) Gray, C. G.; Goldman, S.; Tomberli, B.; Li, W. Comment on "Correlation lengths and density fluctuations in supercritical states of carbon dioxide". *Chem. Phys. Lett.* **1997**, *271*, 185−187.

(48) Matsugami, M.; Yoshida, N.; Hirata, F. Theoretical characterization of the "ridge" in the supercritical region in the fluid phase diagram of water. *J. Chem. Phys.* **2014**, *140*, No. 104511.

(49) Sato, T.; Sugiyama, M.; Itoh, K.; Mori, K.; Fukunaga, T.; Misawa, M.; Otomo, T.; Takata, S. Structural difference between liquidlike and gaslike phases in supercritical fluid. *Phys. Rev. E* **2008**, *78*, No. 051503.

(50) Corradini, D.; Rovere, M.; Gallo, P. The Widom line and dynamical crossover in supercritical water: Popular water models versus experiments. *J. Chem. Phys.* **2015**, *143*, No. 114502.

(51) Fomin, Y. D.; Ryzhov, V. N.; Tsiok, E. N.; Brazhkin, V. V. Dynamical crossover line in supercritical water. *Sci. Rep.* **2015**, *5*, No. 14234.

(52) Brazhkin, V. V.; Fomin, Y. D.; Lyapin, A. G.; Ryzhov, V. N.; Trachenko, K. Universal crossover of liquid dynamics in supercritical region. *JETP Lett.* **2012**, *95*, 164−169.

(53) Bolmatov, D.; Brazhkin, V. V.; Trachenko, K. Thermodynamic behaviour of supercritical matter. *Nat. Commun.* **2013**, *4*, No. 2331.

(54) Brazhkin, V. V.; Fomin, Y. D.; Lyapin, A. G.; Ryzhov, V. N.; Tsiok, E. N.; Trachenko, K. "Liquid-gas" transition in the supercritical region: Fundamental changes in the particle dynamics. *Phys. Rev. Lett.* **2013**, *111*, No. 145901.

(55) Bolmatov, D.; Zhernenkov, M.; Zav'yalov, D.; Stoupin, S.; Cunsolo, A.; Cai, Y. Q. Thermally triggered phononic gaps in liquids at THz scale. *Sci. Rep.* **2016**, *6*, No. 19469.

(56) Kirkwood, J. G.; Buff, F. P. The statistical mechanical theory of solutions. 1. *J. Chem. Phys.* **1951**, *19*, 774−777.

(57) Schofield, P. Wavelength-dependent fluctuations in classical fluids. I. Long wavelength limit. *Proc. Phys. Soc., London* **1966**, *88*, 149−170.

(58) Ploetz, E. A.; Smith, P. E. Local fluctuations in solution mixtures. *J. Chem. Phys.* **2011**, *135*, No. 044506.

(59) Ploetz, E. A.; Smith, P. E. Local fluctuations in solution: Theory and applications. *Adv. Chem. Phys.* **2013**, *153*, 311−372.

(60) Ploetz, E. A.; Karunaweera, S.; Smith, P. E. Experimental triplet and quadruplet fluctuation densities and spatial distribution function integrals for pure liquids. *J. Chem. Phys.* **2015**, *142*, No. 044502.

(61) Ploetz, E. A.; Smith, P. E. Experimental triplet and quadruplet fluctuation densities and spatial distribution function integrals for liquid mixtures. *J. Chem. Phys.* **2015**, *142*, No. 094504.

(62) O'Connell, J. P. Thermodynamic properties of solutions based on correlation functions. *Mol. Phys.* **1971**, *20*, 27−33.

(63) Ben-Naim, A. *Molecular Theory of Solutions*; Oxford University Press: New York, 2006.

(64) Ben-Naim, A. Inversion of the Kirkwood−Buff theory of solutions: Application to the water−ethanol system. *J. Chem. Phys.* **1977**, *67*, 4884−4890.

(65) Smith, P. E.; Matteoli, E.; O'Connell, J. P. *Fluctuation Theory of Solutions: Applications in Chemistry, Chemical Engineering and Biophysics*; CRC Press: Boca Raton, 2013.

(66) Buff, F. P.; Brout, R. Molecular formulation of thermodynamic functions encountered in solution theory. *J. Chem. Phys.* **1955**, *23*, 458−465.

(67) Debenedetti, P. G. Fluctuation simulations and the calculation of mechanical partial molar properties. *Mol. Simul.* **1989**, *2*, 33−53.

(68) Debenedetti, P. G. Fluctuation-based computer calculation of partial molar properties. II. A numerically accurate method for the determination of partial molar energies and enthalpies. *J. Chem. Phys.* **1988**, *88*, 2681−2684.

(69) Debenedetti, P. G. Fluctuation-based computer calculation of partial molar properties. I. Molecular dynamics simulation of constant volume fluctuations. *J. Chem. Phys.* **1987**, *86*, 7126−7137.

(70) Greene, R. F.; Callen, H. B. On the formalism of thermodynamic fluctuation theory. *Phys. Rev.* **1951**, *83*, 1231−1235.

(71) Cummins, H. Z.; Swinney, H. L. Critical opalescence: The Rayleigh linewidth. *J. Chem. Phys.* **1966**, *45*, 4438−4444.

(72) Gray, C. G.; Gubbins, K. E. *Theory of Molecular Fluids. Vol. 1: Fundamentals*; Oxford University Press: New York, 1984.

(73) Chialvo, A. A.; Cummings, P. T. Molecular-based modeling of water and aqueous solutions at supercritical conditions. *Adv. Chem. Phys.* **1999**, *109*, 115−205.

(74) Naleem, N.; Ploetz, E. A.; Smith, P. E. Gaussian and non-gaussian fluctuations in pure classical fluids. *J. Chem. Phys.* **2017**, *146*, No. 094509.

(75) Gubbins, K. E.; Gray, C. G.; Egelstaff, P. A. Thermodynamic derivatives of correlation functions. *Mol. Phys.* **1978**, *35*, 315−328.

(76) Ploetz, E. A.; Pallewela, G. N.; Smith, P. E. Fluctuation Solution Theory of pure fluids. *J. Chem. Phys.* **2017**, *146*, No. 094501.

(77) Wagner, W.; Pruss, A. The IAPWS formulation 1995 for the thermodynamic properties of ordinary water substance for general and scientific use. *J. Phys. Chem. Ref. Data* **2002**, *31*, 387−535.

(78) Tegeler, C.; Span, R.; Wagner, W. A new equation of state for argon covering the fluid region for temperatures from the melting line to 700 K at pressures up to 1000 MPa. *J. Phys. Chem. Ref. Data* **1999**, *28*, 779−850.

(79) Span, R.; Wagner, W. A new equation of state for carbon dioxide covering the fluid region from the triple-point temperature to 1100 K at pressures up to 800 MPa. *J. Phys. Chem. Ref. Data* **1996**, *25*, 1509−1596.

(80) Guder, C.; Wagner, W. A reference equation of state for the thermodynamic properties of sulfur hexafluoride (SF_6) for temper-

atures from the melting line to 625 K and pressures up to 150 MPa. *J. Phys. Chem. Ref. Data* **2009**, *38*, 33−94.

(81) Koga, Y. Chapter VI - Mixing Schemes in Aqueous Solutions of Nonelectrolytes. In *Solution Thermodynamics and its Application to Aqueous Solutions*, 2nd ed.; Koga, Y., Ed.; Elsevier, 2017; pp 199−252.

(82) Koga, Y. The second and higher order derivative thermodynamic quantities and fluctuation functions. *J. Mol. Liq.* **2018**, *249*, 1009−1011.

(83) Mood, A. M.; Graybill, F. A.; Boes, D. C. *Introduction to the Theory of Statistics*, 3rd ed.; McGraw-Hill Book Company: Singapore, 1985.

(84) Widom, B.; Stillinger, F. H. Critical-point thermodynamics of fluids without hole-particle symmetry. *J. Chem. Phys.* **1973**, *58*, 616−625.

(85) Anisimov, M. A.; St. Pierre, H. J. Diverging curvature correction to the interfacial tension in polymer solutions. *Phys. Rev. E* **2008**, *78*, No. 011105.

(86) Anisimov, M. A.; Wang, J. Nature of asymmetry in fluid criticality. *Phys. Rev. Lett.* **2006**, *97*, No. 025703.

(87) Wang, J.; Anisimov, M. A. Nature of vapor-liquid asymmetry in fluid criticality. *Phys. Rev. E* **2007**, *75*, No. 051107.

(88) Wang, J.; Cerdeiriña, C. A.; Anisimov, M. A.; Sengers, J. V. Principle of isomorphism and complete scaling for binary-fluid criticality. *Phys. Rev. E* **2008**, *77*, No. 031127.

(89) Bertrand, C. E.; Nicoll, J. F.; Anisimov, M. A. Comparison of complete scaling and a field-theoretic treatment of asymmetric fluid criticality. *Phys. Rev. E* **2012**, *85*, No. 031131.

(90) Cerdeiriña, C. A.; Anisimov, M. A.; Sengers, J. V. The nature of singular coexistence-curve diameters of liquid−liquid phase equilibria. *Chem. Phys. Lett.* **2006**, *424*, 414−419.

(91) Pérez-Sánchez, G.; Losada-Pérez, P.; Cerdeiriña, C. A.; Sengers, J. V.; Anisimov, M. A. Asymmetric criticality in weakly compressible liquid mixtures. *J. Chem. Phys.* **2010**, *132*, No. 154502.

(92) Anisimov, M. A.; Sengers, J. V.; Levelt Sengers, J. M. H. Near-Critical Behavior of Aqueous Systems. In *Aqueous Systems at Elevated Temperatures and Pressures: Physical Chemistry in Water, Steam and Hydrothermal Solutions*; Palmer, D. A.; Fernandes-Prini, R.; Harvey, A. H., Eds.; Elsevier: Amsterdam, 2004; pp 29−71.

(93) Hill, T. L. *Thermodynamics of Small Systems, Part I*; W. A. Benjamin, Inc: New York, 1963.

(94) Hirschfelder, J. O.; Curtiss, C. F.; Bird, R. B. *Molecular Theory of Gases and Liquids*; Wiley: New York, 1954.

(95) Davidson, N. *Statistical Mechanics*; McGraw-Hill: New York, 1962.

(96) Ploetz, E. A.; Smith, P. E. Classical harmonic model for the behavior of pure fluids at the critical point. *Phys. Chem. Chem. Phys.* **2019**, *21*, 8004−8014.

(97) Kim, Y. C.; Fisher, M. E.; Orkoulas, G. Asymmetric fluid criticality. I. Scaling with pressure mixing. *Phys. Rev. E* **2003**, *67*, No. 061506.

(98) Orkoulas, G.; Fisher, M. E.; Panagiotopoulos, A. Z. Precise simulation of criticality in asymmetric fluids. *Phys. Rev. E* **2001**, *63*, No. 051507.

(99) Hill, T. L. Free-volume models for liquids. *J. Phys. Colloid Chem.* **1947**, *51*, 1219−1232.

(100) Kirkwood, J. G. Critique of the free volume theory of the liquid state. *J. Chem. Phys.* **1950**, *18*, 380−382.

(101) Kirkwood, J. G. Molecular distribution in liquids. *J. Chem. Phys.* **1939**, *7*, 919−925.

(102) Makarevich, L. A.; Sokolova, O. N.; Rozen, A. M. Compressibility of SF_6 along the critical isochore (on the value of the critical exponent gamma). *Sov. Phys. - JETP* **1975**, *40*, 305−307.

(103) Kurzeja, N.; Tielkes, T.; Wagner, W. The nearly classical behavior of a pure fluid on the critical isochore very near the critical point under the influence of gravity. *Int. J. Thermophys.* **1999**, *20*, 531−561.

(104) Ivanov, D. Y. Behavior of critical exponents in the immediate vicinity of a critical point for nonideal systems: The second crossover. *Dokl. Phys.* **2002**, *47*, 267−270.